

Visual Analysis of Longitudinal Brain Tumor Perfusion

Sylvia Glaßer^a, Steffen Oeltze^a, Uta Preim^b, Atle Bjørnerud^c, Helwig Hauser^d and Bernhard Preim^a

^aDepartment of Informatics, University of Magdeburg, Germany

^bMunicipal Hospital of Magdeburg, Germany

^cDepartment of Medical Physics, Rikshospitalet-Radiumhospitalet Medical Centre;
Department of Physics, University of Oslo, Norway

^dDepartment of Informatics, University of Bergen, Norway

ABSTRACT

In clinical research on diagnosis and evaluation of brain tumors, longitudinal perfusion MRI studies are acquired for tumor grading as well as to monitor and assess treatment response and patient prognosis. Within this work, we demonstrate how visual analysis techniques can be adapted to multidimensional datasets from such studies within a framework to support the computer-aided diagnosis of brain tumors. Our solution builds on two innovations: First, we introduce a pipeline yielding comparative, co-registered quantitative perfusion parameter maps over all time steps of the longitudinal study. Second, based on these time-dependent parameter maps, visual analysis methods were developed and adapted to reveal valuable insight into tumor progression, especially regarding the clinical research area of low grade glioma transformation into high grade gliomas. Our examination of four longitudinal brain studies demonstrates the suitability of the presented visual analysis methods and comprises new possibilities for the clinical researcher to characterize the development of low grade gliomas.

Keywords: Brain Tumor Perfusion, Longitudinal Data, Multiple Coordinated View Systems

1. INTRODUCTION

Magnetic resonance imaging (MRI) is used for evaluating brain tumors due to its high soft-tissue contrast. In addition to morphologic aspects represented by conventional MRI, dynamic susceptibility contrast (DSC) perfusion imaging enables the characterization of dynamic aspects, in particular the cerebral microvasculature that is represented by the quantitative perfusion parameter relative cerebral blood volume (rCBV), see Figure 1. DSC-MRI, in combination with conventional MRI, is a good presurgical indicator for glioma grade and may identify the most malignant parts of a tumor for guiding stereotactic biopsy as well as to monitor and assess treatment response and patient prognosis. Gliomas – tumors with a glial cell origin – are the most common primary brain tumors, varying histopathologically from low grade gliomas (LGGs) to high grade gliomas (HGGs).

Grading of gliomas and thus the differentiation between LGGs and HGGs plays an important role for treatment planning and patient outcome.¹ Further, LGGs may transform into HGGs at some point in time, and an early detection of such a transformation is of significant clinical importance. If a surgical removal or radiation treatment is not possible, e.g., due to the tumor’s location or patient’s request, patients with LGGs are commonly subject to a life-long MRI monitoring. Here, the clinical research focus lies on the detection of LGG transformation in longitudinal brain data acquired over several years.

Since tumor growth depends on angiogenesis, i.e., the formation of new vessels and/or the sprouting of existing vessels, the increased cerebral microvasculature yields elevated rCBV values. Evaluation of rCBV is a clinical research focus. It is an important indicator for a patient’s survival and gliomas with high rCBV values have a significantly faster progression time.² Since HGGs have in general foci of higher rCBV values, and rCBV correlates with the tumor grade, rCBV is also employed for differentiation between LGGs and HGGs.^{2–4}

For longitudinal studies, rCBV maps of different acquisitions have to be compared, which is a complex and exploratory analysis task, due to the absence of standardized intensity values and the high variability of MRI

Further author information: glasser@isg.cs.uni-magdeburg.de, Telephone: +49 (0)3 91 67 52 527

scanners and patient data. As one challenge, intervoxel correspondence has to be established between scans of different time steps. This is further complicated by tumor growth and increasing tumor heterogeneity. At last, MRI scans from longitudinal studies are acquired over a period of several years and thus employ different scanning protocols, image resolutions, and sequence parameters. This is in contrast to cohort studies, e.g., the SHIP study,⁵ where many patients are examined in a short time period and extra care is taken to avoid image parameter changes. Currently, longitudinal studies are assessed with software intended for the diagnosis of a patient at one point in time. Hence, no dedicated support for longitudinal studies, i.e., normalization of image data and visual comparison of data from different points in time, is provided.

In this paper, we present a visual analysis approach for the investigation of longitudinal brain tumor perfusion studies within a clinical research scenario. The approach comprises a preprocessing pipeline and the visual analysis framework for the computer-aided evaluation of longitudinal brain tumors. The framework also includes a new 3D parallel coordinates plot that provides a complete overview of all rCBV values at all time steps and allows for fast detection of trends.

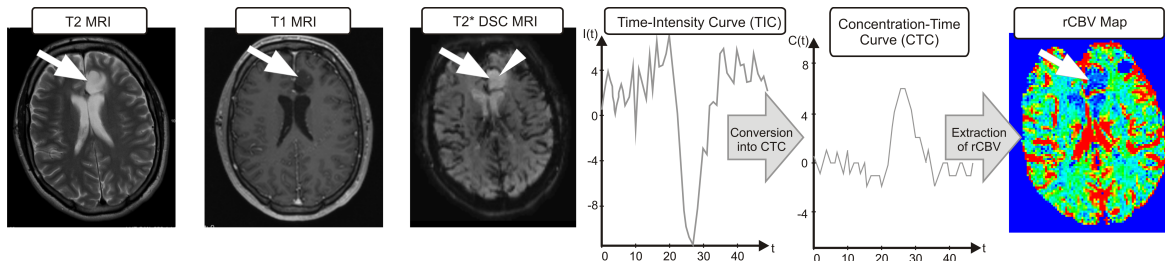


Figure 1. MRI slices with a tumor (see arrow). For a single voxel (see arrowhead) of the DSC-MRI data, the time-intensity curve is extracted and converted into the concentration-time curve (see diagrams). From the concentration-time curve, the parameter CBV is extracted, yielding a CBV map (low values are mapped to blue, high values to red). Note the varying data size, orientation, and image resolution.

2. RELATED WORK

Basic visualization techniques for exploring tumor perfusion data were presented by Behrens et al.,⁶ including color-coded parameter maps. Covarrubias et al.¹ employ rCBV parameter maps to specify ROIs with high rCBV values (also called hot spots), indicating tumor growth and malignancy. Wetzel et al.⁷ analyze different methods for creating a representative ROI regarding intra- and interobserver reproducibility, but a gold standard for a cut-off value between LGGs and HGGs of a ROI's average rCBV value is still missing.⁸ Covarrubias et al.¹ suggest an rCBV value of $1.5 \text{ ml} / 100 \text{ g}$ and Law et al.⁴ $1.75 \text{ ml} / 100 \text{ g}$ as cut-off value. These cut-off values are reported to have high sensitivity but low specificity by Emblem et al.³ They suggest cut-off values between $3.75 - 5.58 \text{ ml} / 100 \text{ g}$ after minimizing the number of glioma grade misclassifications and maximizing the average sensitivity and specificity. Furthermore, Emblem et al. present a histogram analysis of rCBV heterogeneity leading to increased diagnostic accuracy and interobserver agreement. Lupo et al.⁹ extract the spatial heterogeneity of a brain tumor's concentration-time curves to further distinguish microvasculature characteristics.

For scientific visualizations, a 3D parallel coordinates plot has been presented by Wegenkittl et al.¹⁰ The WEAVE system¹¹ links scientific visualizations with multidimensional statistical representations by brushing facilities applied to scatter plots. The SimVis framework¹² extends this work, and was adapted to the visual exploration of perfusion data by Oeltze et al.¹³ Oeltze et al.¹⁴ also analyzed longitudinal ischemic stroke cerebral perfusion data. Kohle et al.¹⁵ introduced an adapted volume rendering of breast MRI data that emphasizes suspicious regions with an appropriate color scheme. Coto et al.¹⁶ present a multidimensional view system with scatter plot-based selections for visual exploration of breast perfusion data, where cutaway views reveal the suspicious breast tumor in its surrounding. Botha et al.¹⁷ present a system for analyzing and exploring medical multi-field data and integrate techniques from pattern analysis to enhance the data exploration process. For visual analysis of breast perfusion data regarding perfusion characteristics and tumor heterogeneity, Glaßer et al.¹⁸ and Preim et al.¹⁹ applied glyphs and region merging.

In clinical research regarding neurological impairments, longitudinal studies are becoming a standard element.²⁰ So far, visual analysis has seen limited use in medical research, although in many applications the magnitude and heterogeneity of the data would strongly benefit from these methods. Steenwijk et al.²¹ apply visual analysis techniques to cohort study image data to explore parameters across patients. In general, there is a wide variety of visual analysis techniques for evaluating *single* perfusion studies. However, specific support for longitudinal studies is needed for the comparison of different points in time – taking into account that imaging parameters may have changed. We want to investigate the applicability of visual analysis techniques to longitudinal perfusion brain studies and investigate rCBV development as well as local tumor heterogeneity approximated with the correlation of rCBV and relative cerebral blood flow (rCBF).²²

3. APPLICATION SCENARIO AND IMAGE DATA

This section introduces clinical research questions regarding LGGs, their development, and the image data for which the visual analysis techniques were developed.

3.1 Clinical Research Questions

The comparison of rCBV maps is the most important question of our clinical partners. As a prerequisite, preprocessing has to be carried out to incorporate rCBV maps from different perfusion scans. Since LGG transformation relates to increased tumor heterogeneity, the evaluation of the tumor’s heterogeneity based on quantitative perfusion parameters is another task. Tumor transformation is also related to tumor growth, which should be visualized. In summary, there are four clinical research question and a last question covering our application that consists of the problem-solving components:

1. How can a comparative rCBV evaluation be achieved for a longitudinal brain perfusion study?
2. When does the LGG transformation start based on the evaluation of rCBV maps?
3. How is the tumor’s heterogeneity characterized in terms of local rCBV and rCBF correlation?
4. How does the tumor grow and develop during the longitudinal study?
5. How can visual exploration and analysis of longitudinal studies be carried out?

3.2 Image Data

Our case study consists of a selection of four patients fulfilling two special conditions: First, each patient had a confirmed diagnosis of an inoperable grade II glioma, i.e., an LGG, and was thus monitored over several years. Second, during this time period, a transformation into an HGG took place. We evaluated the brain MRI data of these four patients resulting in four longitudinal studies $L_1 - L_4$. For each study, up to five MRI protocols including perfusion DSC-MRI sequences, T1 pre- and post-contrast, T2, and Fluid Attenuated Inversion Recovery (FLAIR) MRI were acquired. Typical sequence parameters for the DSC-MRI perfusion studies are gradient-echo echo planar imaging (GRE-EPI) with a temporal resolution $TR = 1.4 - 1.72\text{ s}$, echo time $TE = 30 - 52\text{ ms}$, image matrix $= 128 \times 128$, slice thickness $= 6.5\text{ mm}$, in-plane resolution $= 1.8\text{ mm} \times 1.8\text{ mm}$, number of slices $= 12 - 19$, number of acquisitions $= 50 - 75$, and a total acquisition time ranging from 73 s to 119 s .

For each study, the point in time of the LGG transformation was estimated by an experienced radiologist. The estimation is based on *all* MRI protocols – instead of the single perfusion scan – of all time steps for each study. L_1 was acquired over almost three years at four time steps $t_1 - t_4$ for monitoring of an LGG. The transformation into an HGG started between t_1 and t_2 . The patient of study L_2 underwent surgical intervention and the remaining LGG was monitored for four years. MRI data was acquired at five time steps and the LGG transformation started between t_3 and t_4 . L_3 contains an oligodendroglioma, a glioma type exhibiting foci of high CBV values irrespective of the tumor grade.²³ MRI scans have been acquired at four time steps during two and a half years. The transformation started between t_3 and t_4 . L_4 has been acquired at five time steps to supervise an LGG over a time period of three and a half years. The transformation into an HGG started after t_3 .

4. VISUAL ANALYSIS OF LONGITUDINAL BRAIN TUMORS

Our computer-aided diagnosis of longitudinal brain tumor studies includes two innovations: a *preprocessing pipeline* for the MRI perfusion scans and the *framework* containing the adapted visual analysis techniques.

4.1 Preprocessing Pipeline

Our preprocessing pipeline facilitates the comparison of a longitudinal study’s different perfusion datasets (with possibly different image parameters) and comprises five steps, which are described in the following.

4.1.1 Co-registration of Perfusion Datasets

Motion artifacts in brain perfusion imaging typically result from patient movement. With the skull as static reference object, rigid registration algorithms allow for co-registration of brain perfusion data. We co-registered each study’s perfusion DSC-MRI datasets to the study’s DSC-MRI dataset acquired last in time with *Rview* (rview.colin-studholme.net), employing a rigid registration algorithm.²⁴ Thus, a concurrent analysis of all perfusion scans is supported.

4.1.2 Extraction of CBV and CBF maps

To assess CBV and cerebral blood flow (CBF), the distribution of the contrast agent is analyzed. The contrast enhancement results in time-intensity curves for each voxel (see Fig. 1). We employ the software package *nordicICE* (NordicNeuroLab, www.nordicneurolab.com) to transform these curves into concentration-time curves, applying the regularized singular value decomposition for deconvolution.²⁵ The arterial input function was extracted from the *arteria cerebri media*.²⁶ Contrast agent leakage correction was carried out due to possible contrast agent extravasation in regions of blood-brain-barrier disruption,²⁷ caused by the tumor. CBV is approximated as the area under the concentration-time curve and defined as the total volume of blood traversing a given region of the brain, measured in ml of blood per 100 grams of brain tissue. CBF is defined as the volume of blood traversing a given region of brain per unit time, measured in milliliters of blood per 100 grams of brain tissue per minute. Although in ischemic stroke diagnosis, CBF is thoroughly analyzed, the role of this parameter in brain tumor diagnosis has not been as extensively studied as CBV.¹ We investigate the correlation between CBF and CBV for tumor heterogeneity evaluation. While a small decrease in CBF is expected as a consequence of normal aging in a longitudinal study, the transformation from LGG to HGG is expected to involve significant stronger changes. However, a gold standard for CBF and CBV evaluation seems hard to establish, due to different imaging modalities, age, and gender.⁸

4.1.3 Normalization of CBV and CBF maps

For comparison of CBV and CBF values from DSC-MRI scans, normalization has to be carried out. We employ the general approach, where CBV and CBF maps are normalized with the averaged white matter’s values of the contralateral side,⁷ yielding relative CBV (rCBV) and relative CBF (rCBF) values. Visual inspection and ROI placement are realized with *MeVisLab* (www.mevislab.de), a platform for medical image processing and visualization.

4.1.4 Exclusion of Vessels and Adapted Smoothing

Next, vessels were excluded from the rCBV and rCBF maps, since brain vessels exhibit higher values than the surrounding tissue. They can be identified and removed based on the earlier and stronger contrast enhancement in the DSC-MRI data. We extracted a vessel mask with *nordicICE* based on the cluster analysis of the estimated perfusion-related parameters to separate vessels (both arteries and veins) from other tissue. For each rCBV and rCBF map the corresponding vessel mask is applied. Afterwards, a 3×3 modified average filter is applied to smooth the data as well as to reduce holes caused by the vessel mask. This filter empirically accounts best for rCBV changes due to noise or subtle artifacts. The modified filter only averages over non-vessel voxels in the 3×3 neighborhood of the current filter kernel. Hence, outliers, i.e., isolated voxels with rCBV values higher than a certain threshold, are removed. We employed the .995 quantile of each rCBV map as cut-off value.

4.1.5 Extraction of Tumor Masks

In a last step, a tumor mask for each of the perfusion datasets was created. Hence, the T2 and FLAIR images were co-registered to the perfusion datasets acquired at the same point in time of the studies with Rview. Next, binary tumor masks based on hyperintense areas in T2 and FLAIR data for each study’s time step were extracted and applied to the rCBV maps. Tumor mask creation was manually carried out and validated by an experienced radiologist.

4.2 A Framework for Visual Analysis of Longitudinal Brain Tumors

Based on the preprocessed longitudinal scans, we developed a framework for the longitudinal evaluation of brain perfusion data. The framework contains color-coded 2D and 3D visualizations, a local heterogeneity map, and a parallel coordinates plot view.

4.2.1 Direct 2D and 3D Visualizations

The 2D and 3D visualizations directly map each voxel’s rCBV value to color and are explained in more detail below.

2D rCBV Maps. For direct rCBV extraction, a standard 2D slice view of the brain tumor with voxelwise rCBV is presented. All tumor slices of a study’s scans are provided. We apply a modified rainbow color scale from blue to red, see Figure 2, based on the color scale suggested by Wetzel et al.⁷ Red highlights critical rCBV values (values > 5), and suspicious rCBV values greater than 1 are mapped to cyan. Although rainbow color scales do in general lack an intuitive visual interpretation of the data’s order, they support visual clustering. Hence, regions with mostly red colors (and thus high rCBV values) or blue regions can be observed. Based on the rCBV maps a selection of voxels, – *the rCBV threshold selection* – can be defined. This selection consists of all voxels with an rCBV value greater than a user-defined threshold and can be combined with all other views.

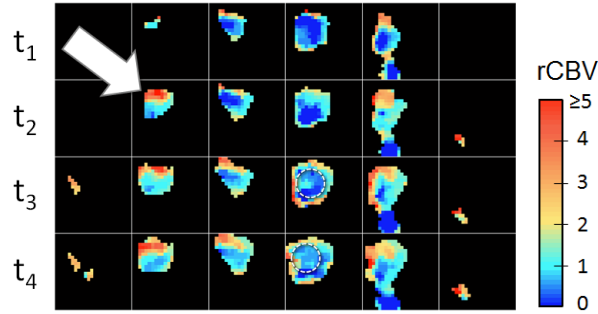


Figure 2. 2D rCBV maps of all slices (horizontally aligned) of study L_1 for all four time steps (vertically aligned) of the study. At t_1 and t_4 , the tumor is covered by four and six slices, respectively. Note the hot spot with high rCBV values (arrow). The encircled regions exhibit lower rCBV values.

3D Overview. The 3D overview provides a direct volume rendering applying the same color scale (see Fig. 2) for highlighting tumor voxels. A linear opacity transfer function assigns α -values of 0.2 to low rCBV values ≤ 1 and $\alpha = 1$ to rCBV values ≥ 5 . The brain (extracted from the perfusion dataset with thresholding) is displayed as isosurface context object and the tumor is revealed by cutting the isosurface, see Figure 3. The 3D overview visualizes the tumor’s progression as well as its spatial localization in the brain. However, only limited information about a tumor’s malignancy can be provided, since no exact quantification of rCBV hot spots is possible. The 3D overview reveals the spatial variability of rCBV hot spots. They may occur at slightly different positions across all scans of a longitudinal study due to tumor growth (see Fig. 3).

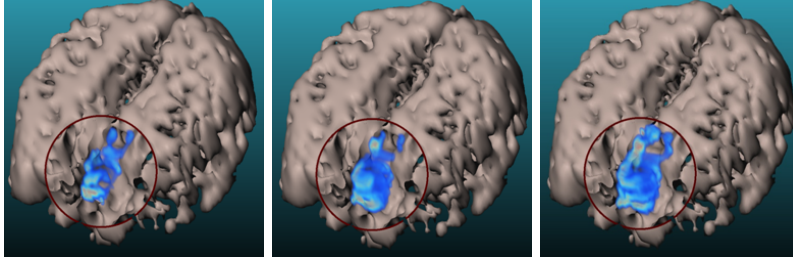


Figure 3. 3D view of tumor growth of L_1 at t_1 (left), t_2 (center), and t_3 (right). The brain is depicted as context object and the tumor is emphasized with a cut-out technique.

4.2.2 Visual Analysis of Local Tumor Heterogeneity

In clinical research, tumor growth and malignancy are associated with increased tumor heterogeneity due to necrosis mainly in the tumor center. Also, some neoangiogenetic tumor parts are expected to exhibit increased heterogeneity. For an assessment of local heterogeneity, approximated as correlation of rCBV and rCBF, we extract the local correlation coefficient (LCC) measure.²⁸ An important property of LCC is the independence of scaling of the data value range. Thus, the LCC maps are independent of rCBV and rCBF normalization factors, which had been used to normalize CBV and CBF maps. We apply LCC to the preprocessed rCBV and rCBF parameter maps, yielding a color-coded 2D LCC parameter map, see Figure 4. LCC values of 1 indicate an increasing linear relationship. Values ≈ 0 illustrate a missing linear dependency. We apply a heat color map from dark red to bright orange to map increasing values of LCC.

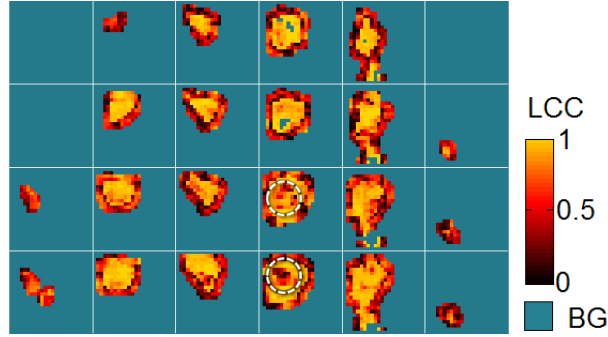


Figure 4. LCC parameter maps of L_1 . Heterogeneous areas are mapped to dark red. The encircled regions at time steps t_3 and t_4 exhibit low rCBV values, see Figure 2.

4.2.3 The rCBV Profile Parallel Coordinates Plot

A parallel coordinates plot allows for the exploration of multivariate data, where each axis presents a data dimension. We adapt the parallel coordinates plot as follows: For each voxel, the rCBV values over time (i.e., the scans at different time steps of a study) are extracted, yielding rCBV curves. In Figure 5, the rCBV profile view of L_1 is presented (the same color scale is applied, recall Fig. 2). According to discussions with our clinical partners, the rCBV changes, i.e., the voxel's rCBV differences between two subsequent time steps were of great interest resulting in the rCBV change profile view, see Fig. 5. Hence, shadows support depth perception, and the rainbow color scale's hue changes support the differentiation between rCBV values. The data's order can be easily inferred from the curves' height. In addition, height lines support direct quantitative rCBV or rCBV change extraction, whereas curve differentiation is supported by contour lines and Fresnel shading.

To obtain groups of similar curves, we tested different strategies to sort the curves. We empirically determined the best result (i.e., the lowest amount of occlusions of curves in the background and the easiest detection of trends) with a sorting based on the squared differences of each rCBV change curve's integral. The order is applied to both rCBV profile views. Tumors with larger extents and thus a larger amount of voxels yield a higher number of rCBV change curves, which may lead to visual clutter. To reduce the curve number, the user

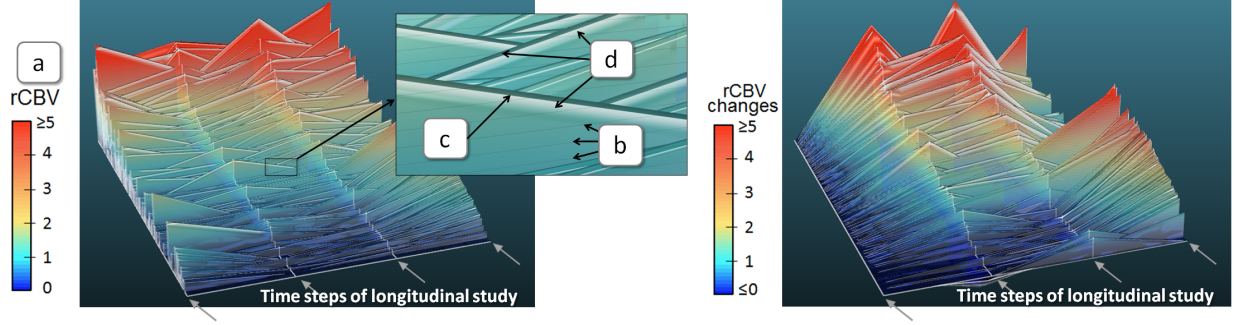


Figure 5. The rCBV profile view (left) with all voxels' rCBV curves. The rCBV values are color-coded (a) and height lines support direct measurement (b). Differentiation of curves is supported by dark contour lines (c), with Fresnel shading attached to (d). The rCBV change profile view presents the rCBV parameter curves' differences (right). Thus, all differences are mapped to zero for t_1 .

can apply the rCBV threshold selection, and only curves that have at least one rCBV value greater than this threshold are included. In addition, the rCBV profile views allow for the *rCBV curve index selection*. Hence, all voxels with a corresponding curve index inside the selected range of curve indices are combined. The curve indices are sorted depending on the rCBV profile view. Although the rCBV profile views allow for simultaneous display of all voxels' rCBV changes, the spatial connectivity of the voxels is lost, as the voxels' order purely depends on the rCBV curves, and not on their spatial position.

4.3 Combination of Visual Analysis Techniques

The presented techniques can be combined via the rCBV threshold selection and the rCBV curve index selection. Then, a tumor voxel is only mapped to color or represented as curve when it is part of all chosen selections. Furthermore, the 2D views can be combined with lenses to allow for simultaneous evaluation of rCBV and LCC values.

5. EVALUATION

In this section, the studies $L_1 - L_4$ were discussed with two physicians regarding the clinical research questions (recall Sec. 3).

5.1 How can a comparative rCBV evaluation be achieved?

With the presented pipeline, a concurrent evaluation of each study's perfusion scans can be achieved. User interaction is only necessary during ROI placement in the contralateral healthy brain tissue. The pipeline can be applied to all brain DSC-MRI datasets independent of MRI scanner or specific scanning protocol parameters. Also, distortion of a ROI's rCBV values due to vessel voxels is prevented.

5.2 When does the LGG transformation start based on the evaluation of rCBV maps?

In general, rCBV maps are evaluated with the hot spot method. If the hot spot's average rCBV value is greater than a certain threshold, e.g., > 1.5 ,¹ the tumor is expected to be an HGG. The transformation of the LGG of L_1 started between t_1 and t_2 , since a hot spot occurs at t_2 with an average rCBV value > 1.5 . The patient of L_2 was monitored after surgical intervention. In Figure 6(a), the development of the recurrent LGG can be observed: First, there is a lesion dominated by radiation necrosis and low rCBV values. Next, the rCBV view at t_4 reveals some rCBV hot spots, whereas at t_5 increased extents of hot spots with higher rCBV are visible. The reported rCBV differences of oligodendrogliomas in comparison to other brain gliomas is reflected by L_3 , since foci with high rCBV values do occur at all time steps (see Fig. 6(e)). Study L_4 comprises an LGG, whereas between t_3 and t_4 more hot spots with increased rCBV values occur, (see Fig. 6(i)). However, in clinical research, it is not always clear at which extent and number of hot spots and which threshold of rCBV a glioma is graded as HGG.^{1,3,4} Furthermore, the normalization of rCBV with a possibly too low or too high normalization factor (extracted on the contralateral brain side) could strongly hamper this analysis and ROI placement suffers from interobserver variability.⁷ These limitations also hold for our parameter maps.

5.3 How is the tumor’s heterogeneity characterized in terms of local rCBV and rCBF correlation?

To support stereotactic biopsy, the most malignant tumor parts have to be determined. These parts are characterized by areas with increased angiogenesis and therefore with highest rCBV values. Furthermore, our clinical research partners presumed increased heterogeneity and thus uncorrelated rCBV and rCBF values for these parts. The LCC maps of L_1 are presented in Figure 4 and of L_2 - L_4 in Figure 6. Hence, also the combination of LCC maps and rCBV maps via lenses is demonstrated. Two facts can be observed: First, with increased tumor growth, heterogeneous areas in the tumor center become visible, which may be caused by necrotic areas. Second, at the tumor’s boundary, uncorrelated areas of rCBV and rCBF exist. During tumor growth, necrotic areas in the tumor center show up with typical low rCBV values, see the encircled regions in Figures 2 and 4. Necrotic tumor parts typically exhibit low rCBV values. For stereotactic biopsy, these parts should be explicitly spared. In contrast, areas with high rCBV and high heterogeneity in terms of LCC should be aimed at. These areas can be defined by applying an rCBV selection first. Next, a ROI is set in the remaining rCBV map (see Fig. 6(c)). Another finding of the LCC maps is the lack of relationship between LGG transformation and the amount of LCC approximated heterogeneity.

5.4 How does the tumor grow and develop?

For a qualitative overview of tumor growth, the 3D view is provided (see Fig. 3, Fig. 6(d)(h)(l)). Hence, no quantitative evaluation is possible. Quantitative information is provided in the 2D parameter maps and the rCBV profile views. Furthermore, the rCBV profile views provide a fast overview of significantly changing rCBV values and thus a possible LGG transformation. This relationship is illustrated in Figure 6(m)-(o), where the rCBV values and the rCBV changes of L_4 suddenly increase after t_3 , matching the estimated transformation point in time. Due to the large tumor extent of L_3 , a reduction of the number of curves is necessary, see Figure 6(p)-(r). Still, no rapid rCBV value increase can be observed due to the oligodendroglioma type.

5.5 How can visual exploration and analysis of longitudinal studies be carried out?

A possible user scenario is carried out in the following way: First, the preprocessing pipeline provides co-registered rCBV parameter maps. Now, the clinical researcher starts with the spatial 3D cut-out view for a first overview. Next, the datasets are analyzed in the rCBV profile curve view and the 2D rCBV maps. Hence, the transformation time step can be estimated by examining the rCBV curves, the rCBV change curves, or scalar values of rCBV. The analysis involves combinations of the rCBV threshold selection and the rCBV curve index selection (see Figures 6((c),(g),(k), and (o)) to determine the most malignant tumor part for tumor grading or stereotactic biopsy.

In summary, for all tumors but the oligodendroglioma of L_3 , the transformation time step (which initially was estimated also based on structural MRI sequences) could be approximated with the application employing only the perfusion datasets (recall Sec. 3.2).

6. CONCLUSION

We presented an application for the evaluation of longitudinal brain perfusion studies focusing on the development of LGGs within the context of clinical research. A preprocessing pipeline enables the simultaneous evaluation of tumor localization, size and rCBV values of all perfusion scans. The visual analysis techniques include linked 2D parameter maps, a 3D overview and the new 3D rCBV profile view that represents all rCBV values of all voxels at all time steps. Once the user examined the LGGs temporal development and the point in time of a starting LGG transformation, the analysis can be restricted to foci with high rCBV values and local tumor heterogeneity. Combination of the different views as well as selecting a set of voxels which may represent the most malignant tumor part is carried out with lenses in the 2D views, the rCBV threshold selection, and the rCBV curve index selection. The resulting voxel set can be used for ROI placement for tumor grading or stereotactic biopsy.

Without our application, a clinician would have to mentally integrate scans of the same study acquired at earlier time steps to evaluate the LGG progression. In addition, the application prevents vessel voxels to be integrated in ROIs and thus avoids distortions of rCBV averaging. Our clinical partners do especially like the rCBV

change profile view depicting each voxel's rCBV changes, due to their ability to visualize the temporal development. Hence, the tumor changes are analyzed for a retrospective evaluation. However, with the heterogeneity analysis based on the LCC, additional information is provided to guide a stereotactic biopsy.

Our framework is a prototype application for clinical research and may be adapted to longitudinal studies of breast and prostate tumors, where perfusion data is acquired for diagnosis and treatment monitoring. Due to the growing number of longitudinal medical image data and the general need of comparison of sequenced image data, e.g., cohort study data, we expect an increasing demand for visual exploration and analysis of this kind of medical data.

Acknowledgements

This work was partially supported by the German Research Foundation project SPP 1335 "Scalable Visual Analytics" and the "Yggdrasil" mobility programme of the Research Council of Norway.

REFERENCES

- [1] Covarrubias, D. J., Rosen, B. R., and Lev, M. H., "Dynamic Magnetic Resonance Perfusion Imaging of Brain Tumors," *Oncologist* **9**(5), 528–37 (2004).
- [2] Law, M., Young, R. J., Babb, J. S., and et al., "Gliomas: Predicting Time to Progression or Survival with Cerebral Blood Volume Measurements at Dynamic Susceptibility-weighted Contrast-enhanced Perfusion MR Imaging," *Radiology* **247**(2), 490–8 (2008).
- [3] Emblem, K. E., Nedregaard, B., Nome, T., and et al., "Glioma Grading by Using Histogram Analysis of Blood Volume Heterogeneity from MR-derived CBV Maps," *Radiology* **247**(3), 808–17 (2008).
- [4] Law, M., Yang, S., Wang, H., and et al., "Glioma Grading: Sensitivity, Specificity, and Predictive Values of Perfusion MR Imaging and Proton MR Spectroscopic Imaging Compared with Conventional MR Imaging," *AJNR* **24**(10), 1989–98 (2003).
- [5] Völzke, H., Alte, D., Schmidt, C. O., and et al., "Cohort Profile: The Study of Health in Pomerania," *International Journal of Epidemiology* **40**(2), 294–307 (2011).
- [6] Behrens, U., Teubner, J., Evertsz, C. J., Walz, M., Jürgens, H., and Peitgen, H.-O., "Computer-Assisted Dynamic Evaluation of Contrast-Enhanced-MRI," in [*Proc. of CARS*], 362–7 (1996).
- [7] Wetzel, S. G., Cha, S., Johnson, G., Lee, P., Law, M., Kasow, D. L., Pierce, S. D., and Xue, X., "Relative Cerebral Blood Volume Measurements in Intracranial Mass Lesions: Interobserver and Intraobserver Reproducibility Study," *Radiology* **224**(3), 797–803 (2002).
- [8] Bjørnerud, A. and Emblem, K. E., "A fully automated method for quantitative cerebral hemodynamic analysis using DSC-MRI," *J Cereb Blood Flow Metab* **30**, 1066–1078 (2010).
- [9] Lupo, J., Cha, S., Chang, S. M., and Nelson, S. J., "Dynamic Susceptibility-Weighted Perfusion Imaging of High-Grade Gliomas: Characterization of Spatial Heterogeneity," *AJNR* **26**(6), 1446–54 (2005).
- [10] Wegenkittl, R., Löffelmann, H., and Gröller, E., "Visualizing the behaviour of higher dimensional dynamical systems," in [*Proc. of IEEE Visualization*], 119–25 (1997).
- [11] Gresh, D. L., Rogowitz, B. E., Winslow, R. L., Scollan, D. F., and Yung, C., "Weave: A system for visually linking 3-d and statistical visualizations, applied to cardiac simulation and measurement data.," in [*Proc. of IEEE Visualization*], 489–92 (2000).
- [12] Doleisch, H., Gasser, M., and Hauser, H., "Interactive Feature Specification for Focus+Context Visualization of Complex Simulation Data," in [*Proc. of the Symposium on Data Visualisation*], 239–48 (2003).
- [13] Oeltze, S., Doleisch, H., Hauser, H., Muigg, P., and Preim, B., "Interactive Visual Analysis of Perfusion Data," *IEEE TVCG* **13**(6), 1392–9 (2007).
- [14] Oeltze, S., Hauser, H., Rørvik, J., Lundervold, A., and Preim, B., "Visual Analysis of Cerebral Perfusion Data – Four Interactive Approaches and a Comparison," in [*Proc. of ISPA*], 588–95 (2009).
- [15] Kohle, S., Preim, B., Wiener, J., and Peitgen, H.-O., "Exploration of Time-varying Data for Medical Diagnosis," in [*Proc. of VMV*], 31–38 (2002).
- [16] Coto, E., Grimm, S., Bruckner, S., Gröller, E., Kanitsar, A., and Rodriguez, O., "Mammo Explorer: An Advanced CAD Application for Breast DCE-MRI," in [*Proc. of VMV*], 91–98 (2005).

- [17] Blaas, J., Botha, C. P., and Post, F. H., "Interactive Visualization of Multi-Field Medical Data Using Linked Physical and Feature-Space Views," in [*IEEE Euro Vis*], 123–30 (2007).
- [18] Glaßer, S., Preim, U., Tönnies, K., and Preim, B., "A Visual Analytics Approach to Diagnosis of Breast DCE-MRI Data," *Computers & Graphics* **34**(5), 602–11 (2010).
- [19] Preim, U., Glaßer, S., Preim, B., Fischbach, F., and Rieke, J., "Computer-Aided Diagnosis in Breast DCE-MRI - Quantification of the Heterogeneity of Breast Lesions," *European Journal of Radiology* **81**(7), 1532 – 1538 (2012).
- [20] Ashburner, J., Csernansk, J. G., Davatzikos, C., Fox, N. C., Frisoni, G. B., and Thompson, P. M., "Computer-assisted imaging to assess brain structure in healthy and diseased brains," *Lancet Neurol* **2**(2), 79–88 (2003).
- [21] Steenwijk, M., Milles, J., Buchem, M., Reiber, J., and Botha, C., "Integrated visual analysis for heterogeneous datasets in cohort studies," in [*IEEE VisWeek Workshop on Visual Analytics in Health Care.*], (2010).
- [22] Netti, P. A., Roberge, S., Boucher, Y., Baxter, L. T., and Jain, R. K., "Effect of transvascular fluid exchange on pressure-flow relationship in tumors: A proposed mechanism for tumor blood flow heterogeneity," *Microvasc Res* **52**(1), 27–46 (1996).
- [23] Lev, M. H., Ozsunar, Y., Henson, J. W., and et al., "Glial Tumor Grading and Outcome Prediction Using Dynamic Spin-Echo MR Susceptibility Mapping Compared with Conventional Contrast-Enhanced MR: Confounding Effect of Elevated rCBV of Oligodendrogliomas," *AJNR* **25**(2), 214–21 (2004).
- [24] Studholme, C., Hill, D. L. G., and Hawkes, D. J., "An overlap invariant entropy measure of 3d medical image alignment," *Pattern Recognition* **32**(1), 71–86 (1999).
- [25] Rosen, B. R., Belliveau, J. W., Vevea, J. M., and Brady, T. J., "Perfusion imaging with NMR contrast agents," *Magn Reson Med* **14**(2), 249–65 (1990).
- [26] Østergaard, L., Weisskoff, R. M., Chesler, D. A., Gyldensted, C., and Rosen, B. R., "High resolution measurement of cerebral blood flow using intravascular tracer bolus passages. Part I: mathematical approach and statistical analysis," *Magnetic Resonance in Medicine* **36**(5), 715–25 (1996).
- [27] Boxerman, J. L., Schmainda, K. M., and Weisskoff, R. M., "Relative cerebral blood volume maps corrected for contrast agent extravasation significantly correlate with glioma tumor grade, whereas uncorrected maps do not," *AJNR* **27**(4), 859–67 (2006).
- [28] Cachier, P. and Pennec, X., "Non-rigid registration by gradient descent on a gaussian-windowed similarity measure using convolutions," in [*Proc. of MMBIA*], 182–9 (2000).

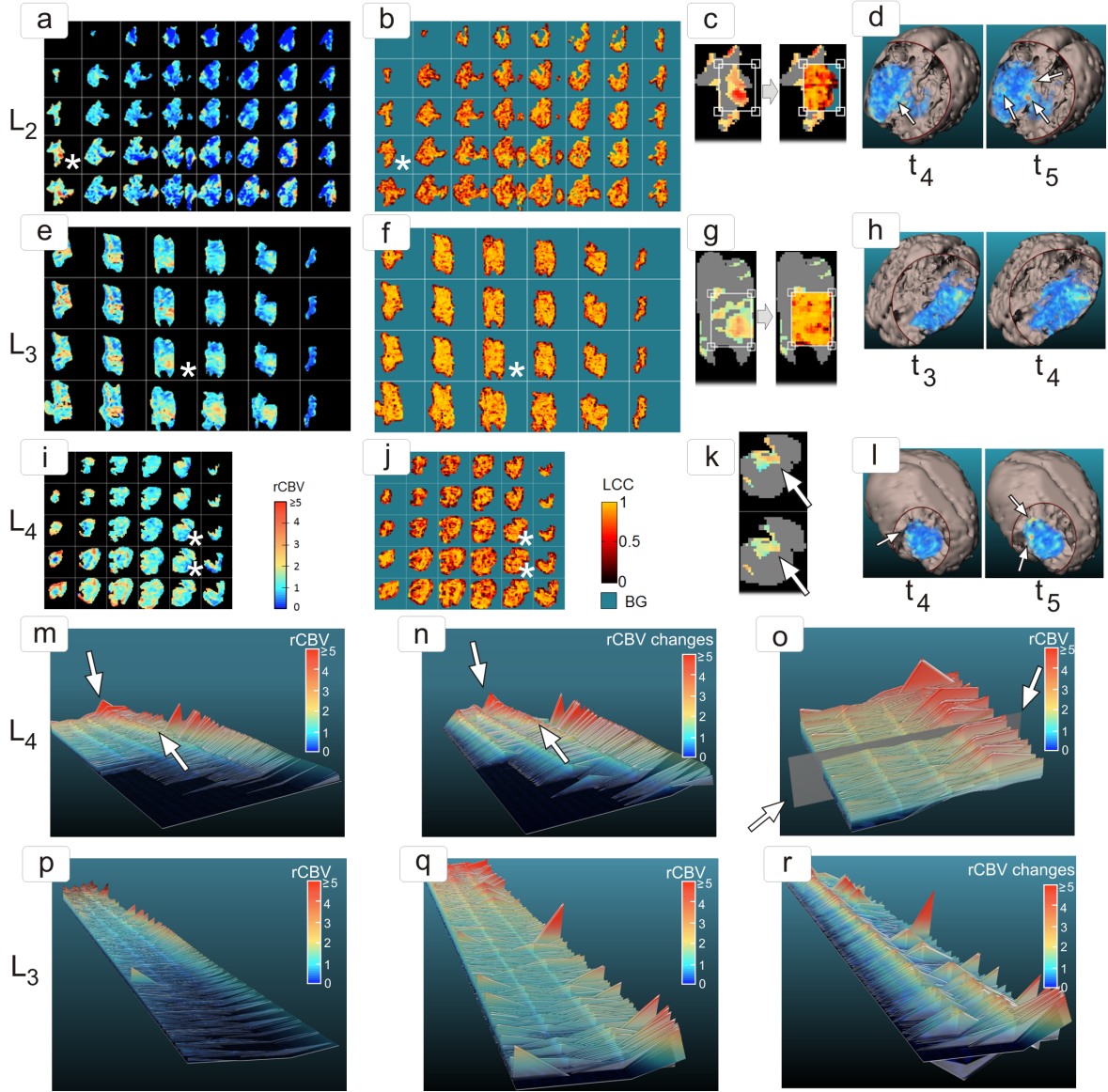


Figure 6. Presentation of the visual analysis techniques applied to L_2 - L_4 . To improve readability, the first and the last 2 tumor slices of L_2 and L_3 are not presented. In (a), (e) and (i) the rCBV maps with corresponding LCC maps in (b), (f), and (j) are depicted. In (d), (h), and (l), the 3D overviews are presented.

The combination of (a) and (b) via a lens for a selected slice (marked with *) is depicted in (c), revealing a hot spot with increased local heterogeneity at the tumor's boundary. In (a) and (d), increased rCBV values and larger hot spots (marked with arrows) at t_4 and t_5 are revealed. In (g), the combination of (e) and (f) via a lens for a selected slice (marked with *) is depicted, revealing a hot spot with increased local heterogeneity in the tumor's center. In (c) and (g), the rCBV threshold selection (rCBV threshold = 1.5) is applied, mapping lower rCBV values to gray. In (k), the rCBV curve index selection is applied to the slices marked with * in (i). Only the voxels, which were selected in the rCBV profile view in (o), are mapped to color. The region marked with an arrow exhibits only moderate rCBV, but these voxels belong to the selected curve indices. Thus, this tumor part may be one of the most malignant parts, since these voxels correspond to rCBV curves with the highest curve indices, i.e., the highest integrals. The rCBV profile view (m) and the rCBV change profile view (n) reveal increased rCBV values and changes, marked with arrows, after t_3 – matching the estimated transformation starting time. In (o), an rCBV curve index selection is carried out by applying the selection plane (see arrows) such that from the 600 rCBV curves with highest integral 300 curves are selected. The selection is then applied to all other views, see the rCBV map in (k).